Supplementary Figures

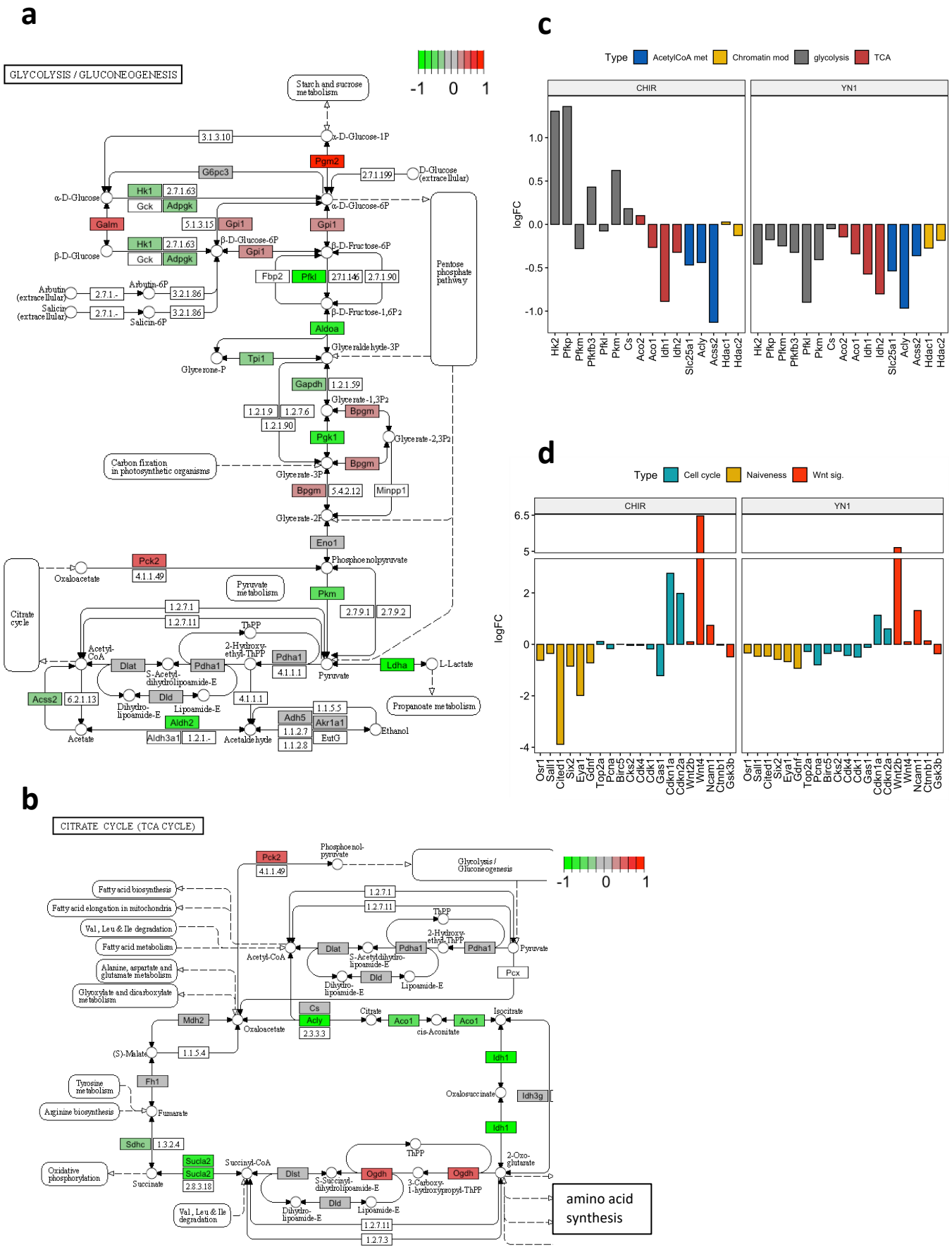
a
GLYCOLYSIS / GLUCONEOGENESIS
-1 0 1
Starch and sucrose metabolism
α-D-Glucose-1P
Pgm2
G6pc3
D-Glucose (extracellular)
α-D-Glucose
Hk1
Gck
Adpgk
α-D-Glucose-6P
Galm
Gpi1
β-D-Glucose-6P
β-D-Fructose-6P
Pentose phosphate pathway
Fbp2
Pfkl
β-D-Fructose-1,6P2
Arbutin (extracellular)
Arbutin-6P
Salicin (extracellular)
Salicin-6P
Aldoa
Glyceraldehyde-3P
Glycerone-P
Tpi1
Gapdh
Glycerate-1,3P2
Bpgm
Pgk1
Glycerate-2,3P2
Carbon fixation in photosynthetic organisms
Glycerate-3P
Minpp1
Glycerate-2P
Eno1
Phosphoenolpyruvate
Pck2
Oxaloacetate
Pyruvate metabolism
Pkm
Citrate cycle
Acetyl-CoA
Dlat
Pdha1
2-Hydroxyethyl-ThPP
S-Acetyldihydrolipoamide-E
Pyruvate
Ldha
L-Lactate
Acss2
Dihydrolipoamide-E
Dld
Lipoamide-E
Propanoate metabolism
Acetate
Aldh2
Aldh3a1
Acetaldehyde
Adh5
Akr1a1
EutG
Ethanol
b
CITRATE CYCLE (TCA CYCLE)
Phosphoenolpyruvate
Glycolysis / Gluconeogenesis
Fatty acid biosynthesis
Fatty acid elongation in mitochondria
Val, Leu & Ile degradation
Fatty acid metabolism
Alanine, aspartate and glutamate metabolism
Glyoxylate and dicarboxylate metabolism
ThPP
Acetyl-CoA
S-Acetyldihydrolipoamide-E
Dihydrolipoamide-E
Pcx
Cs
Acly
Citrate
Aco1
Isocitrate
cis-Aconitate
Mdh2
Oxaloacetate
(S)-Malate
Idh1
Tyrosine metabolism
Fh1
Arginine biosynthesis
Fumarate
Oxalosuccinate
Idh3g
Sdhc
Oxidative phosphorylation
Sucla2
Succinyl-CoA
Succinate
Dlst
S-Succinyldihydrolipoamide-E
Ogdh
3-Carboxy-1-hydroxypropyl-ThPP
2-Oxoglutarate
Val, Leu & Ile degradation
amino acid synthesis
c
Type
AcetylCoA met
Chromatin mod
glycolysis
TCA
CHIR
YN1
logFC
Hk2 Pfkp Pfkm Pfkfb3 Pfkl Pkm Cs Aco2 Aco1 Idh1 Idh2 Slc25a1 Acly Acss2 Hdac1 Hdac2
d
Type
Cell cycle
Naiveness
Wnt sig.
CHIR
YN1
logFC
Osr1 Sall1 Cited1 Six2 Eya1 Gdnf Top2a Pcna Birc5 Cks2 Cdk4 Cdk1 Gas1 Cdkn1a Cdkn2a Wnt2b Wnt4 Ncam1 Ctnnb1 Gsk3b

Fig.S1: Molecular characterization of transcriptomes from YN1 and CHIR-treated NPC. To visualize changes in gene expression, the LogFC values between YN1-treated NPCs and control NPCs were scaled between -1 (green, downregulated), 0 (grey, no change), and +1 (red, upregulated), and the scores were plotted on the KEGG Glycolysis/Gluconeogenesis (a), KEGG citrate cycle (b). LogFC values, representing the gene expression changes between YN1-treated and control NPCs for genes associated with acetyl-CoA production and metabolism, were plotted for multiple genes. These values were color-coded according to their pathway signature (c). LogFC values, representing the gene expression changes between YN1-treated and control NPCs for genes associated with cell cycle (gold), NPC naiveness (cyan), or WNT signaling (red) were plotted for multiple genes (d). Source data are provided as a Source Data file.

a

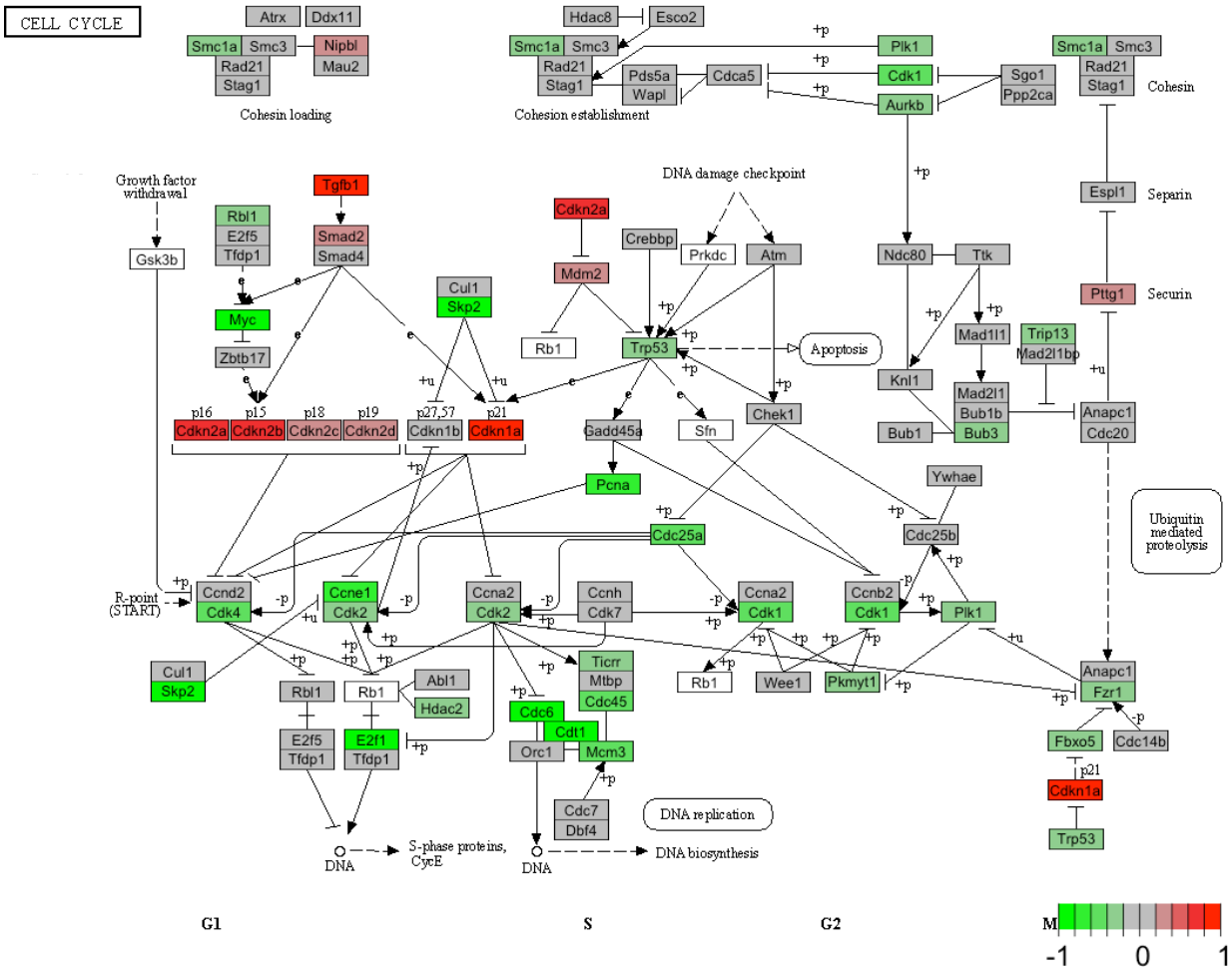
CELL CYCLE
Cohesin loading
Cohesion establishment
Cohesin
Separin
Securin
DNA damage checkpoint
Growth factor withdrawal
Apoptosis
Ubiquitin mediated proteolysis
R-point (START)
DNA
S-phase proteins, CycE
DNA biosynthesis
DNA replication
G1
S
G2
M
-1
0
1

b

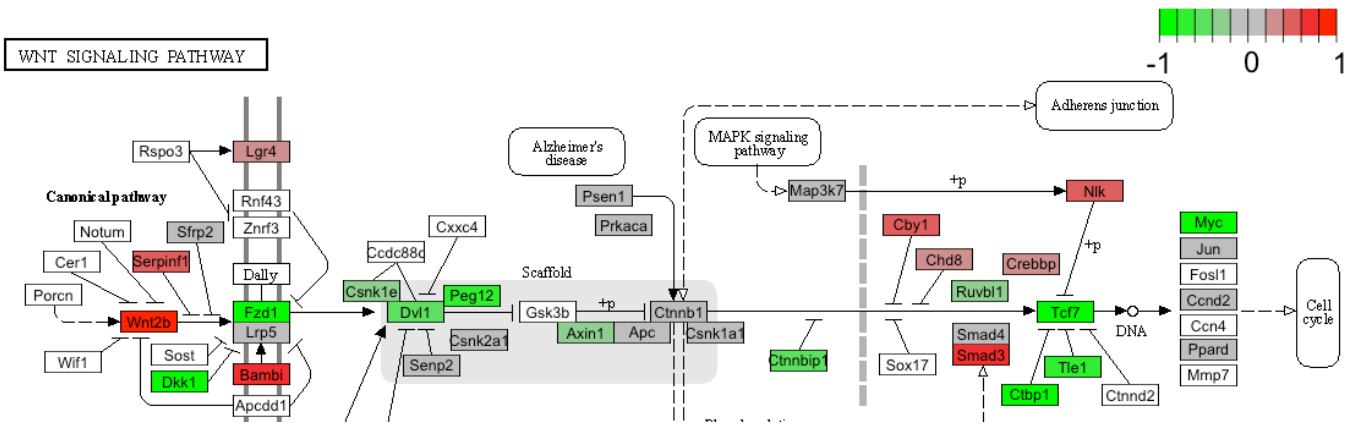
WNT SIGNALING PATHWAY
-1
0
1
Canonical pathway
Scaffold
Alzheimer's disease
MAPK signaling pathway
Adherens junction
DNA
Cell cycle

Fig.S2: Impact of YN1 treatment on cell cycle genes and WNT signaling. LogFC values depicting gene expression changes between YN1-treated NPCs and control NPCs were normalized to a color scale ranging from -1 (green, downregulated) to +1 (red, upregulated). These values were then visualized on the KEGG cell cycle pathway (a) and KEGG WNT signaling pathway (b). Notably, the figure highlights the activation of cell cycle inhibitors, including p21 (highlighted in red oval), and a reduction in several genes of the intracellular WNT machinery following YN1 treatment. Source data are provided as a Source Data file.

a

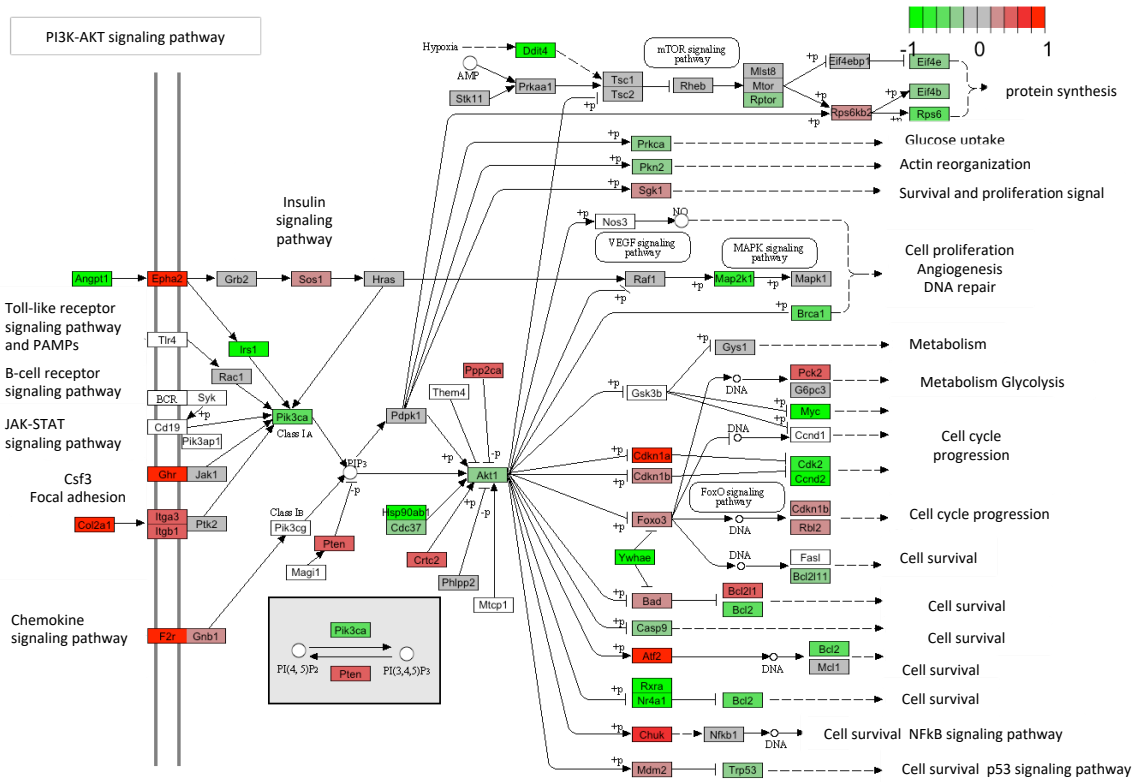
PI3K-AKT signaling pathway
-1
0
1
Hypoxia
AMP
Ddit4
Stk11
Prkaa1
mTOR signaling pathway
Tsc1
Tsc2
Rheb
Mtor
Mist8
Rptor
Eif4ebp1
Eif4e
Eif4b
Rps6kb2
Rps6
protein synthesis
Glucose uptake
Actin reorganization
Survival and proliferation signal
Prkca
Pkn2
Sgk1
Insulin signaling pathway
Nos3
NO
VEGF signaling pathway
MAPK signaling pathway
Cell proliferation
Angiogenesis
DNA repair
Angpt1
Epha2
Grb2
Sos1
Hras
Raf1
Map2k1
Mapk1
Brca1
Toll-like receptor signaling pathway and PAMPs
B-cell receptor signaling pathway
JAK-STAT signaling pathway
Csf3
Focal adhesion
Chemokine signaling pathway
Tlr4
Irs1
Rac1
BCR
Syk
Cd19
Pik3ap1
Ghr
Jak1
Itga3
Itgb1
Ptk2
Col2a1
F2r
Gnb1
Pik3ca
Class IA
Class IB
Pik3cg
PIP3
Pdpk1
Akt1
Ppp2ca
Them4
Pten
Magi1
Hsp90ab1
Cdc37
Crtc2
Phlpp2
Mtcp1
PI(4, 5)P2
PI(3,4,5)P3
Gys1
Metabolism
Gsk3b
Pck2
G6pc3
Metabolism Glycolysis
Myc
Ccnd1
Cell cycle progression
Cdkn1a
Cdkn1b
Cdk2
Ccnd2
FoxO signaling pathway
Foxo3
Cdkn1b
Rbl2
Cell cycle progression
Ywhae
Fasl
Bcl2l11
Cell survival
Bad
Bcl2l1
Bcl2
Cell survival
Casp9
Cell survival
Atf2
Bcl2
Mcl1
Cell survival
Rxra
Nr4a1
Bcl2
Cell survival
Chuk
Nfkb1
Cell survival NFkB signaling pathway
Mdm2
Trp53
Cell survival p53 signaling pathway
DNA

b

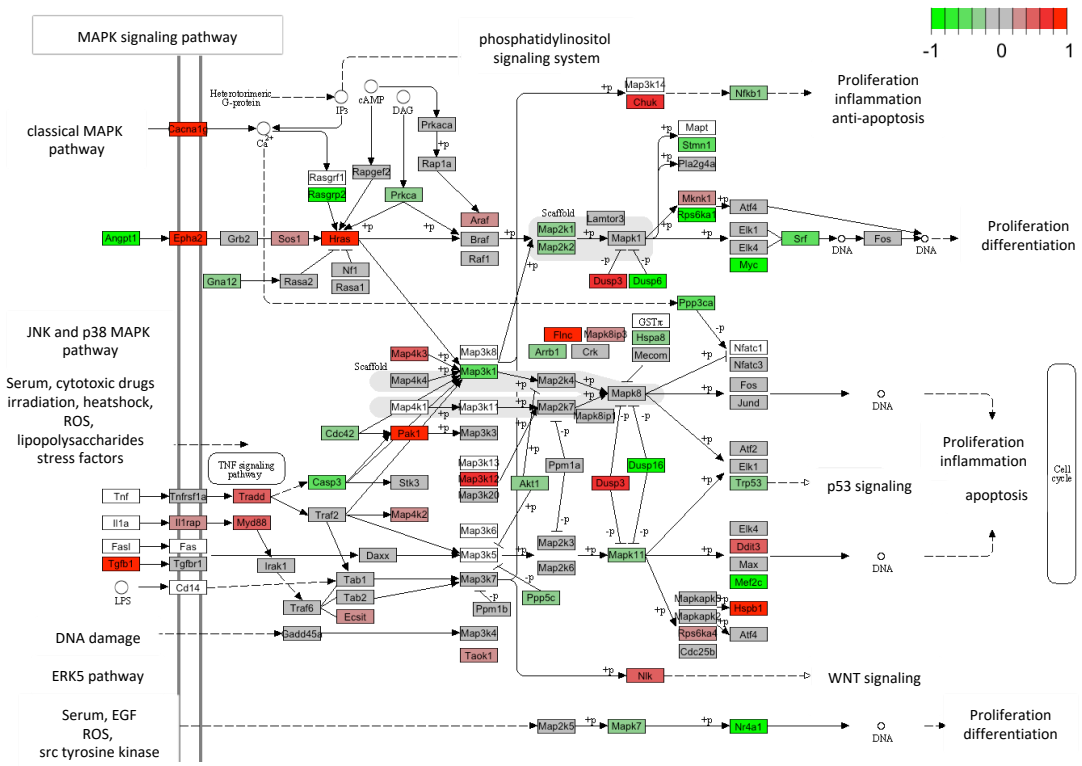
MAPK signaling pathway
phosphatidylinositol signaling system
-1
0
1
classical MAPK pathway
JNK and p38 MAPK pathway
Serum, cytotoxic drugs irradiation, heatshock, ROS, lipopolysaccharides stress factors
DNA damage
ERK5 pathway
Serum, EGF ROS, src tyrosine kinase
Heterotrimeric G-protein
IP3
cAMP
DAG
Prkaca
Ca2+
Cacna1g
Rasgrf1
Rasgrp2
Rapgef2
Rap1a
Angpt1
Epha2
Grb2
Sos1
Hras
Araf
Braf
Raf1
Gna12
Rasa2
Nf1
Rasa1
Scaffold
Map2k1
Map2k2
Lamtor3
Mapk1
Dusp3
Dusp6
Mknk1
Rps6ka1
Atf4
Elk1
Elk4
Srf
Fos
Myc
DNA
Proliferation differentiation
Ppp3ca
GSTπ
Hspa8
Mecom
Flnc
Mapk8ip1
Arrb1
Crk
Map4k3
Map4k4
Map4k1
Map3k8
Map3k1
Map3k3
Map3k13
Map3k14
Map3k15
Map3k20
Map3k6
Map3k5
Map3k7
Map3k4
Taok1
Cdc42
Pak1
Ppm1a
Akt1
Dusp16
Dusp3
Mapk8
Mapk8ip1
Map2k4
Map2k7
Map2k3
Map2k6
Mapk11
Ppp5c
Ppm1b
Mapkapk5
Mapkapk3
Rps6ka4
Cdc25b
Hspb1
Atf4
Nfkb1
Chuk
Mapt
Stmn1
Pla2g4a
Proliferation inflammation anti-apoptosis
Nfatc1
Nfatc3
Fos
Jund
Atf2
Elk1
Trp53
p53 signaling
Elk4
Ddit3
Max
Mef2c
Proliferation inflammation apoptosis
Cell cycle
TNF signaling pathway
Tnf
Tnfrsf1a
Tradd
Casp3
Stk3
Traf2
Map4k2
Il1a
Il1rap
Myd88
Fasl
Fas
Tgfb1
Tgfbr1
Irak1
Daxx
Cd14
LPS
Tab1
Tab2
Traf6
Ecsit
Gadd45a
Nlk
WNT signaling
Map2k5
Mapk7
Nr4a1
Proliferation differentiation

Fig.S3: PI3K and MAPK pathways response to YN1 treatment. LogFC values depicting gene expression changes between YN1-treated NPCs and control NPCs were normalized to a color scale ranging from -1 (green, downregulated) to +1 (red, upregulated). These values were then visualized on the KEGG PI3K-AKT signaling pathway (a) and MAPK signaling pathway (b). The figure highlights a reduction in key elements in these pathways such as PI3K catalytic subunit and AKT1. Source data are provided as a Source Data file.

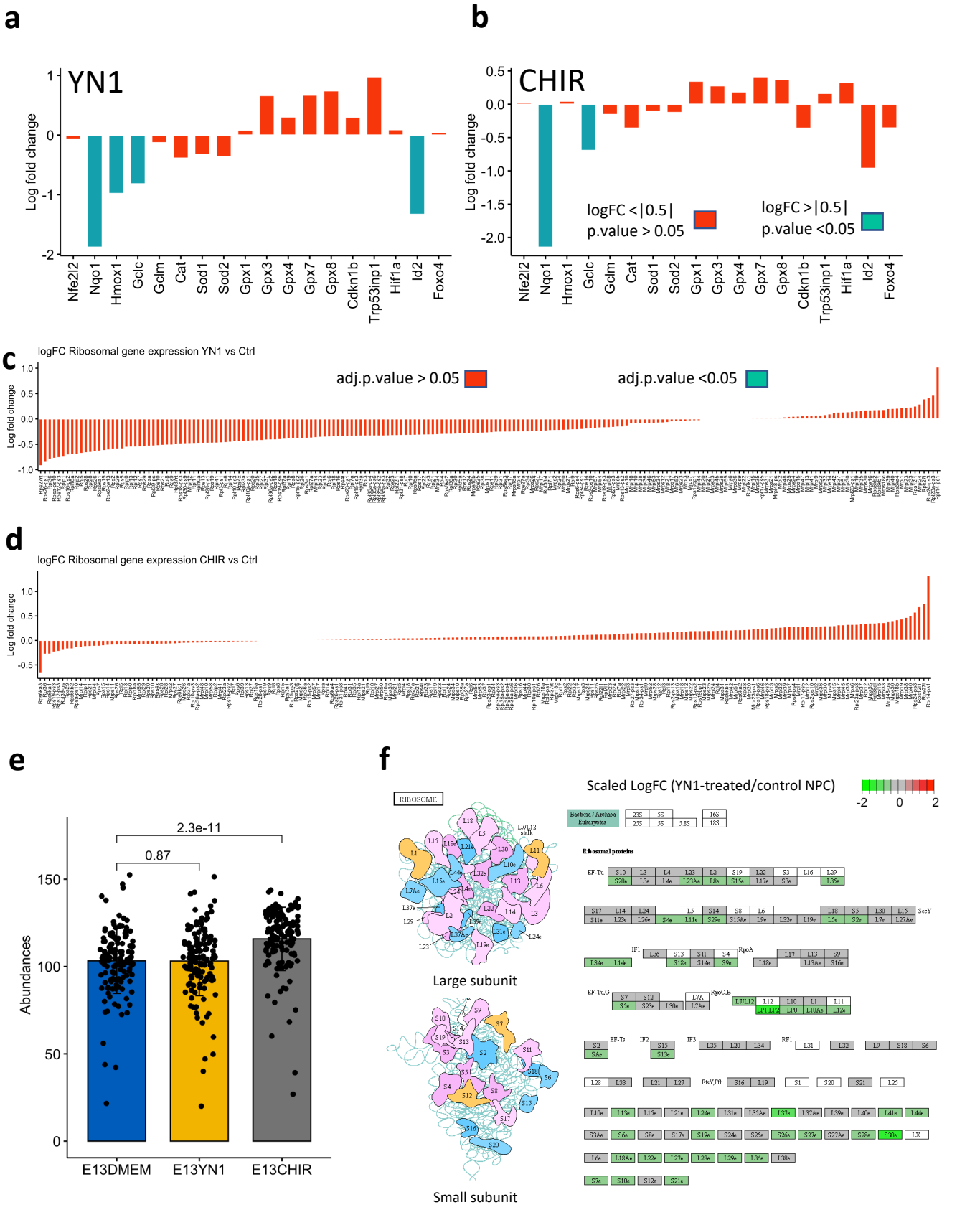
a
YN1
Log fold change
Nfe2l2
Nqo1
Hmox1
Gclc
Gclm
Cat
Sod1
Sod2
Gpx1
Gpx3
Gpx4
Gpx7
Gpx8
Cdkn1b
Trp53inp1
Hif1a
Id2
Foxo4
b
CHIR
logFC <|0.5|
p.value > 0.05
logFC >|0.5|
p.value <0.05
c
logFC Ribosomal gene expression YN1 vs Ctrl
adj.p.value > 0.05
adj.p.value <0.05
d
logFC Ribosomal gene expression CHIR vs Ctrl
e
2.3e-11
0.87
Abundances
E13DMEM
E13YN1
E13CHIR
f
RIBOSOME
Large subunit
Small subunit
Scaled LogFC (YN1-treated/control NPC)
Ribosomal proteins

Fig.S4: Evaluation of stress oxidative response and protein synthesis in the transcriptome of YN1 and CHIR-treated NPC. The LogFC values of genes associated with the oxidative stress response were compared between YN1-treated and control NPCs (a), or CHIR-treated and control NPCs (b) and color-coded based on their LogFC and p-value variation. Only LogFC variations greater than |0.5| and p-values less than 0.05 were considered significant. The LogFC values of ribosomal protein-coding gene expression after YN1 (c) and CHIR (d) treatment are shown. Differences in the abundance of ribosomal proteins after treatment with either YN1 or CHIR compared to control NPC (e). The Kruskal-Wallis test was used for the comparisons across groups and p-values are shown in the figure. To visualize changes in ribosomal protein-coding gene expression, the LogFC values were scaled between YN1-treated NPCs and control NPCs and color-coded as green (downregulated), grey (no change), or red (upregulated), with a scale ranging from -1 to +1. These scores were then plotted on the KEGG Ribosomal pathway (f). Source data are provided as a Source Data file.

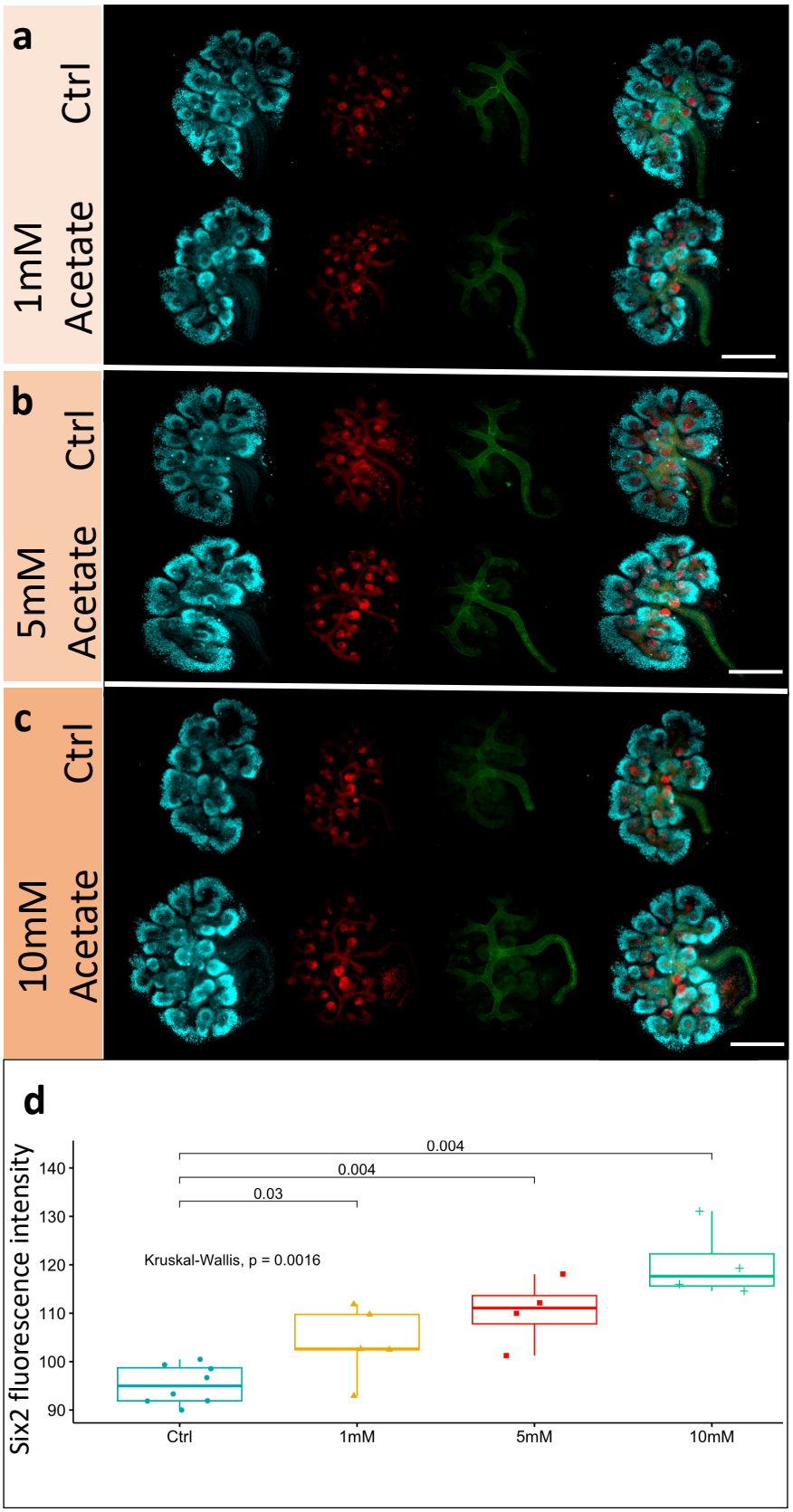
a
Ctrl
1mM Acetate
b
Ctrl
5mM Acetate
c
Ctrl
10mM Acetate
d
Six2 fluorescence intensity
140
130
120
110
100
90
0.004
0.004
0.03
Kruskal-Wallis, p = 0.0016
Ctrl
1mM
5mM
10mM

Fig.S5: Sodium acetate treatment increases CM size. E12.5 mouse kidneys were incubated for 24h in the presence or absence of 1 mM (a), 5 mM (b), or 10 mM sodium acetate (c) and probed with antibodies against Six2 (nephron progenitor cells, Cyan), Lhx1 (nascent nephrons, Red) or DBA (ureteric bud, green). Quantification of Six2 antibody staining, control kidneys n = 8, kidneys treated with sodium acetate 1mM n = 5; 5 mM n = 4; 10 mM n =5) (d). Scale bar 250 µm. Differences between groups were tested with the Kruskal-Wallis test, and Dunn's test for pairwise multiple comparisons, and p-values are reported. Source data are provided as a Source Data file.

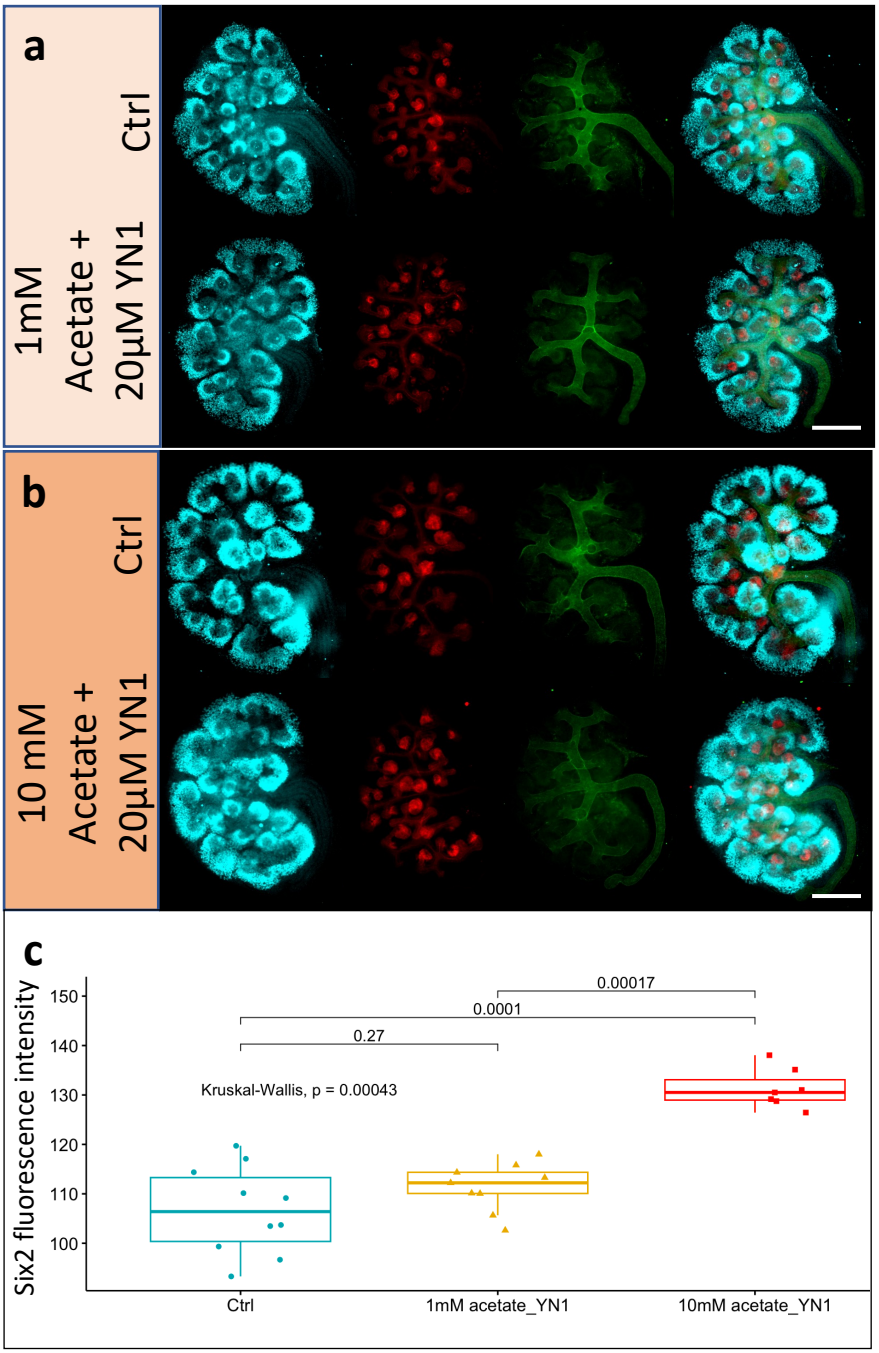
a
Ctrl
1mM Acetate + 20µM YN1
b
Ctrl
10 mM Acetate + 20µM YN1
c
Six2 fluorescence intensity
150
140
130
120
110
100
0.00017
0.0001
0.27
Kruskal-Wallis, p = 0.00043
Ctrl
1mM acetate_YN1
10mM acetate_YN1

Fig.S6: Sodium acetate treatment prevents the YN1 effect on developing kidneys. E12.5 mouse kidneys were incubated for 24h in the presence of 20 μM YN1 + either 1 mM (a) or 10 mM sodium acetate (b) and probed with antibodies against Six2 (nephron progenitor cells, Cyan), Lhx1 (nascent nephrons, Red) or DBA (ureteric bud, green). Quantification of Six2 antibody staining, control kidneys n = 10, kidneys treated with sodium acetate 1mM n = 10; 5 mM n = 4; 10 mM n =7) (c). Control kidneys were incubated with vehicle only, scale bar= 250 μm. Differences between groups were tested with the Kruskal-Wallis test, and Dunn's test for pairwise multiple comparisons, and p-values are reported. Source data are provided as a Source Data file.

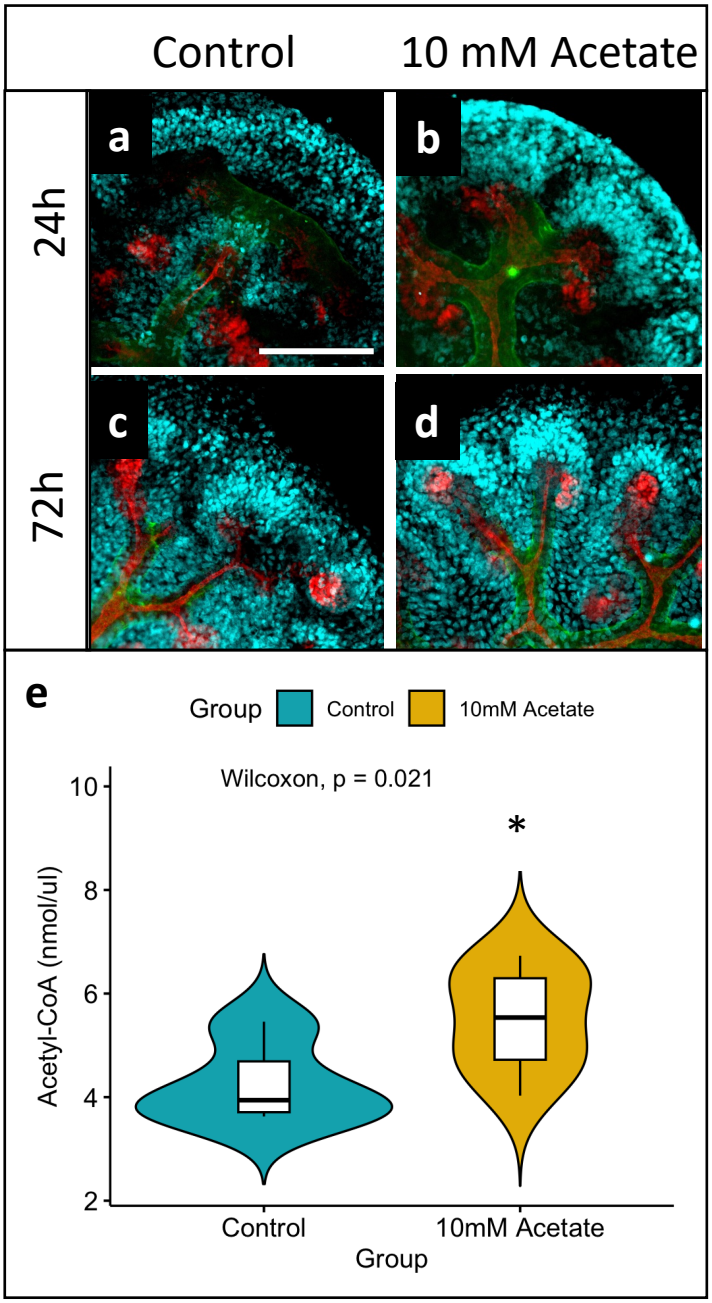
Control
10 mM Acetate
24h
72h
a
b
c
d
e
Group
Control
10mM Acetate
Wilcoxon, p = 0.021
*
Acetyl-CoA (nmol/ul)
10
8
6
4
2
Control
10mM Acetate
Group

Fig.S7: Effects of prolonged exposure to sodium acetate on developing kidneys. E12.5 mouse kidneys were incubated for 24 hours in vehicle (a) or 10 mM sodium acetate (b). E12.5 mouse kidneys were incubated for 72 hours in vehicle (c) or 10 mM sodium acetate (d). Samples were probed with antibodies against Six2 (nephron progenitor cells, cyan), Lhx1 (nascent nephrons, red), or DBA (ureteric bud, green), n = 6 pairs of E12.5 embryonic kidneys per experimental group. The culture media was changed daily until the time of collection at 24 or 72 hours. Scale bar: 100 μm. Sixteen pairs of E12.5 mouse kidneys were incubated for 24 hours in the presence of vehicle or 10 mM sodium acetate, and the cytosolic acetyl-CoA accumulation was measured at the end of the incubation time as described in Methods (e). Differences between groups were tested using the Wilcoxon Rank Sum test with a p-value reported. Source data are provided as a Source Data file.

Ctrl *Acly$^{F/+}$;Six2Cre$^{-/-}$*	Het *Acly$^{F/+}$;Six2Cre$^{+/-}$*	Mut *Acly$^{F/F}$;Six2Cre$^{+/-}$*
a 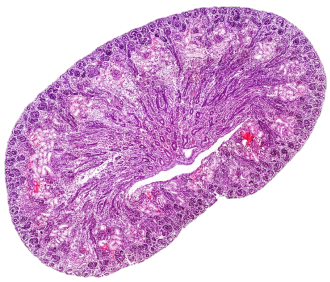	**b** 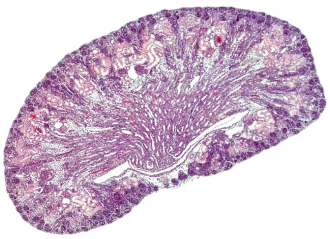	**c** 
d 	**e** 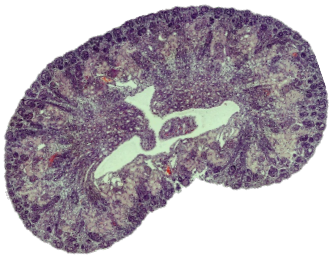	**f** 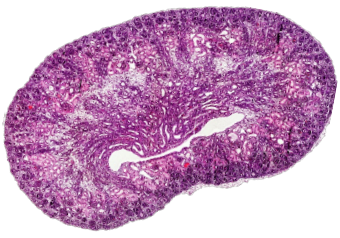
g 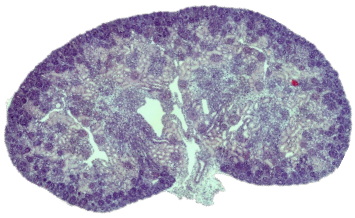	**h** 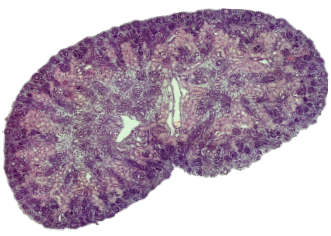	**i** 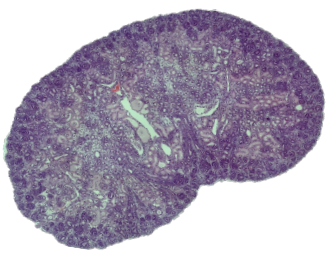
j 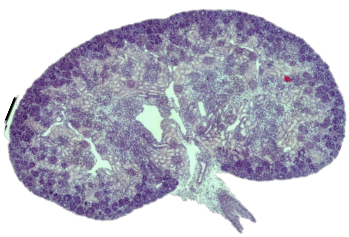	**k** 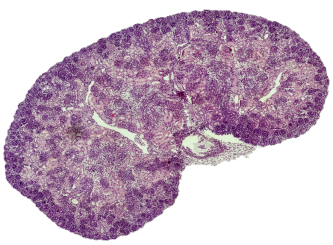	**l** 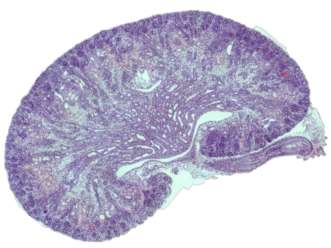

Fig.S8: Morphological characterization of P0 wild type, heterozygous and mutant kidneys lacking *Acly* in Six2-expressing cells. H&E staining of P0 *Acly*$^{F/+}$*;Six2Cre*$^{-/-}$ (control) kidneys (a,d,g,j). H&E staining of P0 *Acly*$^{F/+}$*;Six2Cre*$^{+/-}$ (heterozygous) kidneys (b,e,h,k). H&E staining of P0 *Acly*$^{F/F}$*;Six2Cre*$^{+/-}$ (mutant) kidneys (c,f,i,l). Notice mutant kidneys with narrower nephrogenic zones and fewer nascent nephrons. N = 4 kidneys per genotype displayed.

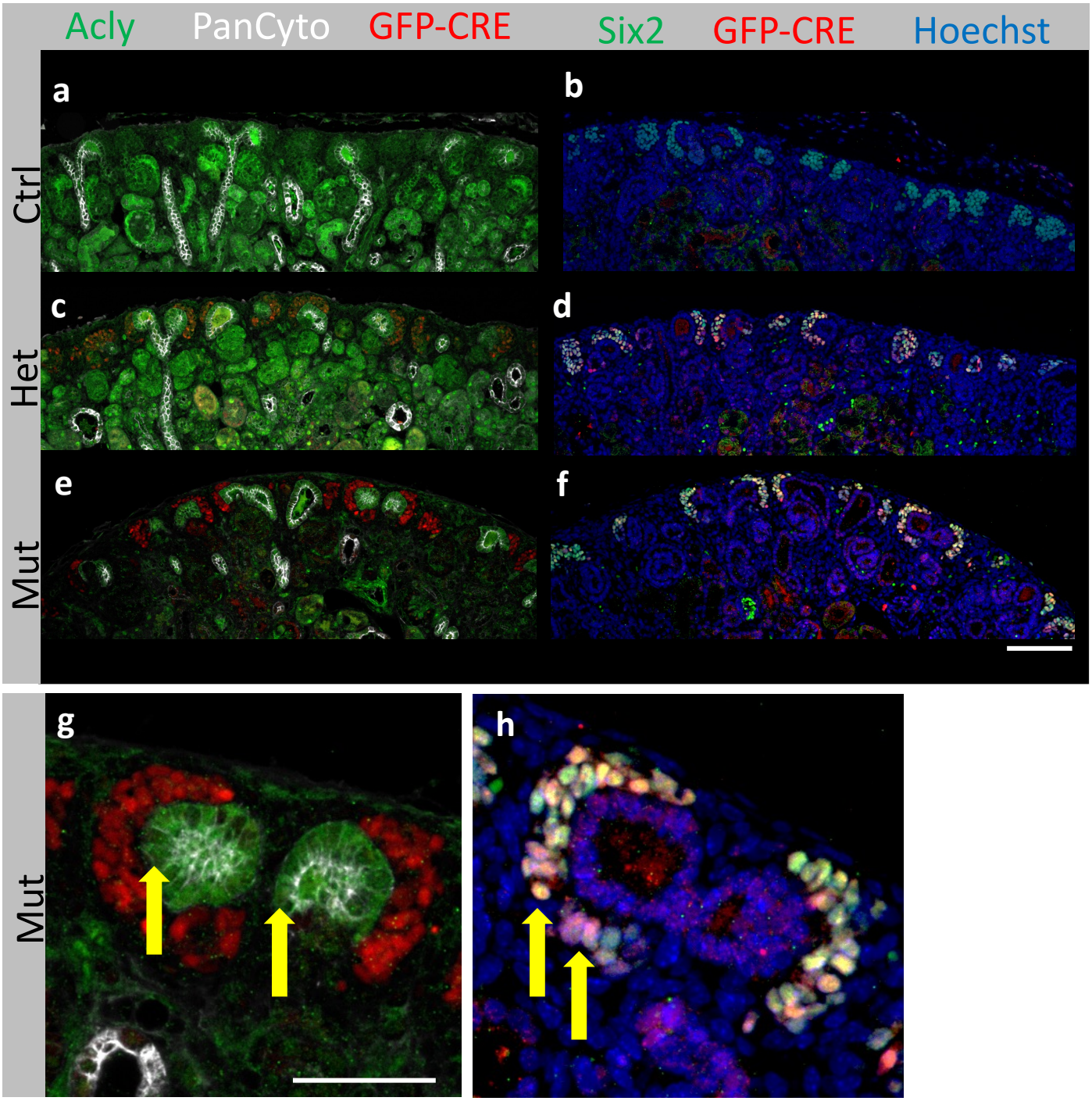
Acly
PanCyto
GFP-CRE
Six2
GFP-CRE
Hoechst
Ctrl
Het
Mut
a
b
c
d
e
f
Mut
g
h

Fig.S9: Removal of Acly from Six2^{+} cells eliminated Acly from the entire nephrogenic lineage. P0 AclyF/+;Six2Cre-/- (control, n=6) kidneys (a,b), P0 AclyF/+;Six2Cre+/- (heterozygous, n=6) kidneys (c,d), and P0 AclyF/F;Six2Cre+/- (mutant n=5) kidneys (e,f) were collected, and analyzed by immunostaining to confirm efficient Acly removal from nephrogenic lineage. Antibodies used and color codes are depicted in the figure. Efficient Acly removal was observed in the mutant kidney (e,f) as evidenced by the absence of green (Acly) signal in the nephrogenic lineage. However, the green (Acly) signal was still present in the UB lineage, and it colocalized with the UB marker Pan cytokeratin (g, yellow arrows). The Cre transgene expression exclusively colocalized with the Six2+ cells (h, yellow arrows), which confirmed the specificity and efficiency of Acly recombination in NPC. A-F scale bar = 250 μm, g,h scale bar = 100 μm. Nuclear staining was carried out with Hoechst 33342.

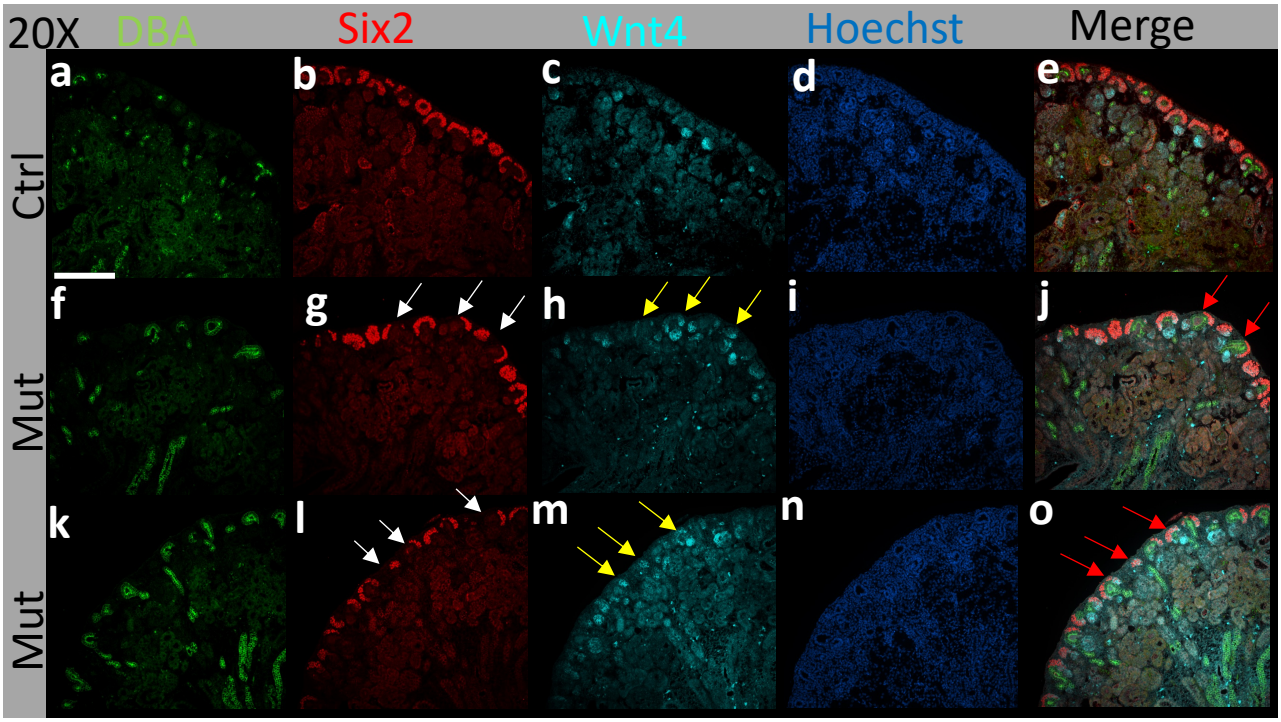
20X
DBA
Six2
Wnt4
Hoechst
Merge
Ctrl
Mut
Mut
a
b
c
d
e
f
g
h
i
j
k
l
m
n
o

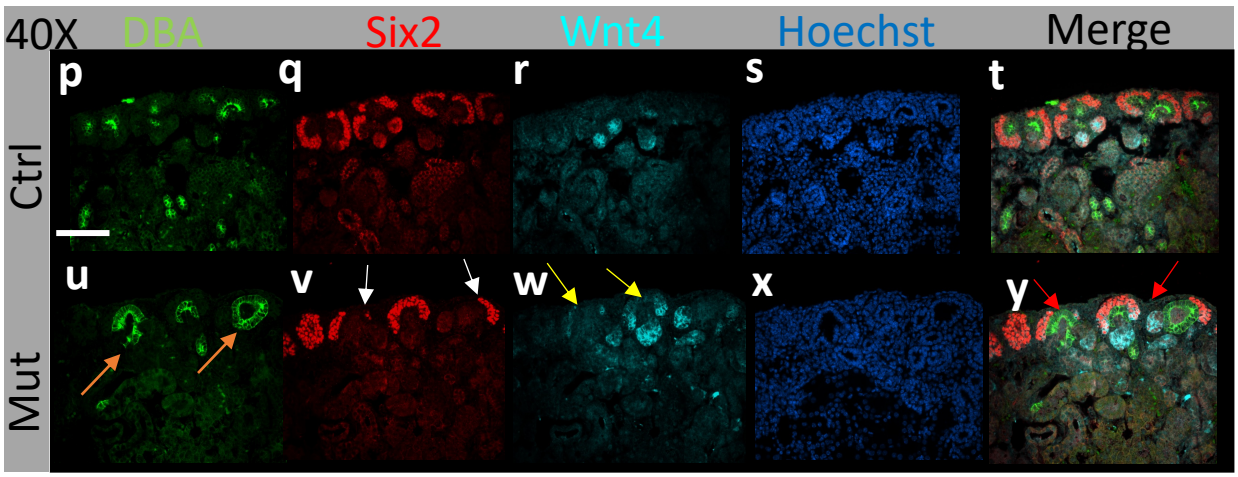
40X
DBA
Six2
Wnt4
Hoechst
Merge
Ctrl
Mut
p
q
r
s
t
u
v
w
x
y

Fig.S10: Immunofluorescence staining of kidney developmental makers in Acly mutant CM at P0. 20X visualization of the nephrogenic zone of control kidneys (Ctrl) (a-e) and two mutant kidneys (f-o) lacking expression of *Acly* in the CM (Mut, mutant kidney). Orange arrows point to dilated UB ampullae; white arrows show areas with depleted cap-mesenchyme; yellow arrows show expansion of Wnt4 towards the cap-mesenchyme. Red arrows show areas co-stained with Wnt4 and Six2 antibodies. On the second panel, a 40x close-up of Ctrl (p-t) and Mut (u-y). These experiments were repeated with at least 5 kidneys per genotype with similar results. UB was stained with DBA (green); CM was stained with Six2 antibody (Red); nascent nephrons and differentiating NPC were stained with Wnt4 (Cyan); Nuclear staining was carried out with Hoechst 33342 (blue). Scale bar a-o = 500 μm; p-y scale bar = 250 μm.

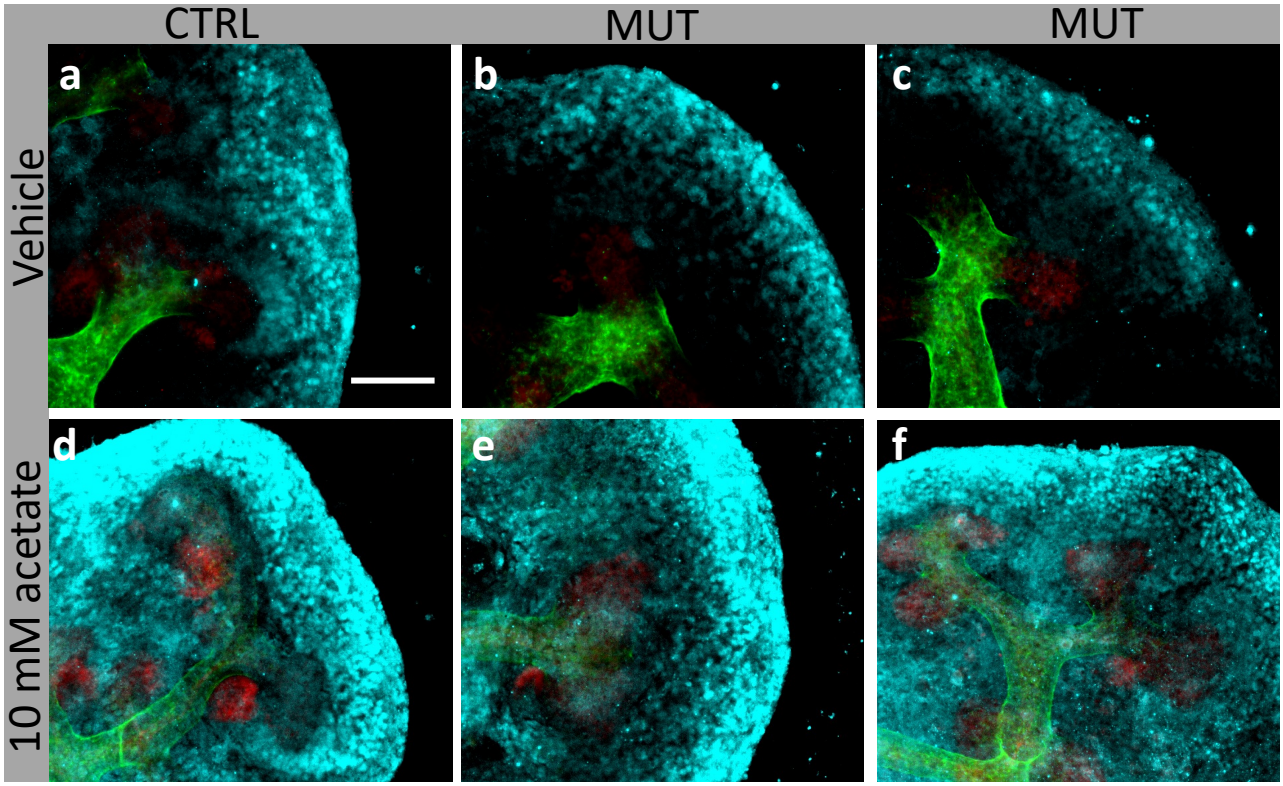
CTRL
MUT
MUT
Vehicle
10 mM acetate
a
b
c
d
e
f

Fig.S11: Acetate supplementation is sufficient to rescue CM size in kidneys lacking *Acly* in Six2-expressing cells. Five pairs of kidneys from control (CTRL) and mutant (MUT) embryos at E12.5 were cultured for 24 hours with either vehicle (a, b, c) or 10 mM sodium acetate (d, e, f). Sodium acetate prevented CM depletion observed in the mutant embryos (compare a to b and c) and promoted CM expansion in both control and mutant embryos (d to f). The immunostaining was performed using antibodies against Six2 (nephron progenitor cells, cyan), Lhx1 (nascent nephrons, red), and UB (DBA, green). The figure shows 1/5 control and 2/5 mutant kidneys. Scale bar 100 μm.